

## THERMAL PHENOMENA IN THE FRICTION PROCESS OF THE TG15 - HARD ANODIC COATING COUPLE

The paper presents a one-dimensional model of heat conduction in a couple consisting of a cylinder made of a sliding plastic material, TG15, and a cuboid made of alloy AW 6061 coated with a hard anodic coating, where the couple is heated with the heat generated during friction. TG15 is a composite material based on polytetrafluoroethylene (PTFE) with a 15% graphite filler, used for piston rings in oil-free air-compressors. Measurement of temperature in the friction zone is extremely important for the understanding and analysis of the phenomena occurring therein. It is practically impossible to introduce a temperature sensor in such a place. Therefore, the interaction taking place in such a couple was modelled using numerical methods. In order to simplify and accelerate the calculations, a one-dimensional model and constant thermophysical parameters of the materials participating in friction were adopted. To solve the proposed model, the finite difference method was used (FDM). The resultant system of equations was solved by means of an explicit scheme.

*Keywords:* hard anodic coating, plastic materials, oil free couples, friction heat, numerical simulation

### 1. Introduction

The conditions of a sliding interaction, i.e. normal load ( $P$ ) and relative velocity ( $v$ ), determine the working conditions, and thus the amount of the generated heat. Friction heat induces an increase in the average temperature of the interacting parts and a local growth of temperature in the area of their actual contact. The amount of the emitted heat depends on the type of the elementary friction processes and the effort made by the parts. The type of friction predominating in an interacting couple depends on the chemical composition and surface topography of the bodies subject to friction, while unit pressures and relative velocity determine the quantity of the heat generated. In the friction process, part of the effort turns into heat.

Increasing temperature usually decreases material strength, while increasing its plasticity. For instance, aluminium alloys with silicon, AC 47000 (Mahle 124), used for the manufacture of pistons of combustion engines, at a temperature of 20°C have  $R_m=200-250$  MPa, which falls to 40-65 MPa at the operating temperature of the piston crown (350°C) [1]. This is of decisive importance, especially in the case of a sliding interaction of an alloy coated with an anodic, very hard ceramic coating (AHC) with a thickness of up to 100  $\mu$ m. Decreasing strength of the alloy causes a decrease of resistance of the coating to concentrated load. This is very important in combustion engines in which pistons are used with an AHC reaching the first ring, if hard impurities, such as the accumulated carbon deposit, gets in between the piston and cylinder sleeve. A decreased alloy strength will lead to its further plastic deformation, exceeding the permissible deformation

of the anodic hard coating which, in turn, will start cracking and its chips will only intensify the wear.

In the case of an interaction between an alloy coated with an AHC and plastic materials which, during friction, create a sliding film consisting of friction products on the surface of the coating, the thermal properties are of different importance. The thickness of the sliding film depends on a number of factors, including mainly:

- temperature of softening of the plastic material deposited on the contact surface of the interacting parts,
- the heat flux generated in the contact zone,
- surface topography of the interacting parts, and
- adhesion of the plastic material to the coating.

The discussed couple: plastic material/anodic hard coating, has found its application in the construction of an oil free piston air compressor in which, as a result of air compression, the temperature of the cylinder sleeve may reach 130°C. The temperature has a significant influence on the properties of the plastic material, including the film applied onto the bearing surface of the cylinder sleeve. As the temperature grows, the shear strength of the plastic material decreases, which causes a decrease of the friction coefficient. Therefore, examination of the temperature distribution resulting from the friction heat will allow understanding the conditions of formation of a sliding film and of the change of friction forces in the oil free couple: sliding plastic material/ceramic anodic coating.

Sliding contacts of polymers, understood as friction couples in which at least one component is made of a plastic material, are more and more frequently used in the machine building industry [2, 3]. The most common plastic materials used

\* UNIVERSITY OF SILESIA, DEPARTMENT OF MATERIALS SCIENCE, 10 ŻYTNA STR., 41-200 SOSNOWIEC, POLAND

\*\* SILESIA UNIVERSITY OF TECHNOLOGY, DEPARTMENT OF AUTOMOTIVE VEHICLE SERVICE, 8 KRASIŃSKIEGO STR., 40-019 KATOWICE, POLAND

# Corresponding author: grzegorz.sluzalek@us.edu.pl

for the production of sliding parts in machines are PTFE based composites with a graphite additive or polyurethane/polyacetal based composites containing PTFE as solid lubricant. Newer solutions propose polyurethane and polyetheretherketone based composite plastic materials reinforced with glass fibre and modified with solid lubricants [2], interacting with composite ceramic coatings modified with solid lubricants [3]. Composite materials containing carbon nanotubes or glassy carbon particles, which play the role of solid lubricants, offer new possibilities of shaping the tribological properties of oil free couples [4].

Pure PTFE is also distinguished by high creep under load, low hardness and poor heat conductivity. These properties considerably reduce the range of applications of this material. Modification through the application of different fillers, such as metal powders, graphite, carbon fibre or glass, changes its properties in the desirable direction. Graphite enhances an increase of compressive and shear strength, as well as hardness and resistance to wear. Due to its low friction coefficient and good thermal conductivity ( $\lambda=120-140$  W(mK) for industrial graphites [5-6]), it is particularly recommended for operation under conditions of technically dry friction (friction in air). An addition of 15% graphite to PTFE significantly reduces its abrasive wear and friction coefficient.

## 2. Experiment - experimental test

Tribological tests were performed for TG15 (PTFE+15% graphite by weight). It is a sliding plastic used for example for contacts which needs to carry out of electric charge generated during friction, for example piston rings in gas compressor. This material is characterised by following properties [7]: density  $2140$  kg/m<sup>3</sup>,  $R_m \approx 12$  MPa, coefficient of friction with most partners  $\mu \approx 0.12$  and  $0.08$  against anodic hard coating, coefficient of thermal expansion  $CTE=14 \times 10^{-5}/K$ .

Cylinder-shaped specimens with diameter  $d=11.2$  mm (friction surface of the specimen:  $1$  cm<sup>2</sup>) and length  $l=20$  mm were made through mechanical processing. Counter-specimens with an anodic coating formed on aluminium alloy EN-AW AlMg2 (6061) through hard anodizing were cut out from a 4 mm thick sheet metal. The counter-specimens had a width of 20 mm and length of 200 mm.

Properties of anodic coatings obtained on aluminium and its alloys may change in a broad range, depending on the production process parameters, the composition of electrolyte, the composition and structure of the substrate, and the type of finishing. The produced anodic coatings are very hard when compared to the basic metal. Their microhardness measured with Vickers method amounts to  $500-600$   $\mu$ HV [3, 8, 9]. High resistance to abrasive wear plays a significant role in numerous applications of anodic coatings deposited on the working surfaces of sliding parts of machines.

Tribological tests were conducted at a test stand presented in Fig. 1. A scheme of the sliding contact is presented in Fig. 2. Fig. 3 shows the surface of a specimen and the surface morphology of the counter-specimen before the interaction, as

well as the AHC before the interaction and with the deposited sliding polymer film.

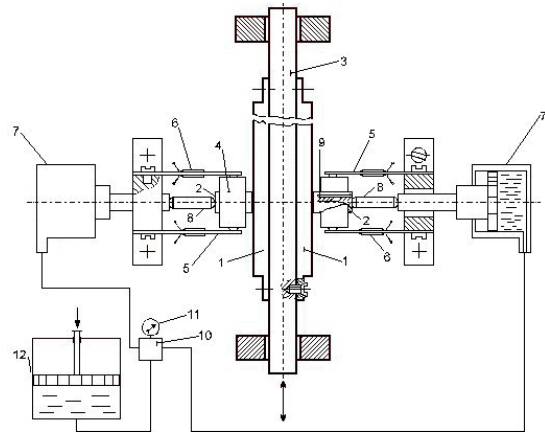


Fig. 1. Scheme of the tribological tester: 1 - counter-specimen: prism  $20 \times 4 \times 200$  mm (tested AHC on aluminium alloy 6061); 2 - specimen: cylinder  $11.2$  mm (TG15); 3 - slide way; 4 - hinged specimen holder; 5 - force sensor; 6 - strain gauge bridge; 7 - hydraulic cylinder; 8 - hinged pusher; 9 - bore for temperature sensor; 10 - 4/2 manipulator; 11 - pressure gauge; 12 - hydraulic pump

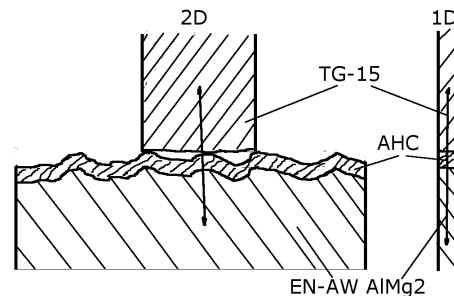


Fig. 2. Model of the sliding contact of the tribological tester and the flow of heat for a one-dimensional (1D) and two-dimensional (2D) system

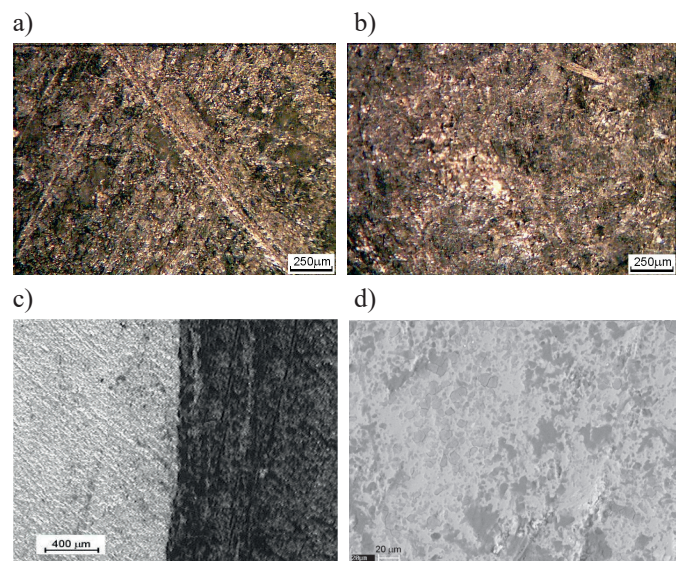


Fig. 3. View of the surface of the specimen and counter-specimen: a) and b) TG15 before a sliding interaction; c) anodic hard coating before the interaction (left side and with an applied sliding film (dark part of the right side)); d) a magnified fragment with an applied sliding film

### 3. Model formulation and its qualitative description

The process of heat emission during friction is connected with the formation and destruction of structure in the surface layer of the bodies undergoing friction. The core of the problem of heat emission consists in the fact that the source of heat covers a certain region located at a given depth under the surface. The depth of the internal heat source changes with changing friction conditions, reaching values from micrometres to a few millimetres.

The analytical models known from professional literature [10-14] did not allow obtaining distributions of the temperature field with characteristic maxima under the surface. Therefore, a necessity appeared to develop a model which would enable obtaining temperature curves consistent with the experiment.

This paper presents a one-dimensional model generating a temperature field of bodies subject to friction. The presented solution may constitute a starting point for the analysis of processes encompassing the distribution of temperature fields taking into account the phenomena which accompany friction.

Development of a numerical simulation of the temperature field of bodies undergoing friction was performed on the basis of data obtained from authors' measurements.

The following test conditions were adopted:

- technically dry friction
- unit pressure:  $p=0.25\text{MPa}$ ,
- average linear sliding velocity:  $v=1.2\text{ m/s}$ ,
- friction coefficient:  $\mu=0.08$ ,
- movement of a specimen in relation to counter-specimen: reciprocating motion,
- cylindrical specimen with a dimension  $d=11.2\text{ mm}$  and length  $l=20\text{ mm}$ .

The formulation of the model was preceded with the following assumptions:

- the form of the heat source function depends on the friction process parameters (loads, dimensions and types of materials, bodies subject to friction and linear speed),
- transport of heat takes place through conduction,
- external surfaces cool down to the ambient temperature, in accordance with third-type boundary conditions

Calculations of the internal heat source as a function of time and of the temperature field of components heated as a result of friction were performed based on the Kirchhoff-Fourier heat condition differential equation [15-16]. For the purpose of numerical simulation, the heat condition differential equation must be solved taking into account the internal heat source (1):

$$c_i * \rho_i * \frac{\delta T_i}{\delta t} + q = \nabla(\lambda * \nabla T_i) \quad (1)$$

where:

T - initial temperature of the interacting parts (i)

t - time of interaction of the couple,

c - specific heat of the materials of the interacting parts (i),

$\rho$  - density of the investigated materials (i),

$\delta$  - partial derivative

$\nabla$  - Hamilton operator,

$\lambda$  - heat conduction coefficient of the materials of the interacting parts (i),

i - 1=(EN-AW AlMg2 (6061)), 2= anodic hard coating, 3= TG15.

The flux of the heat generated during friction, transferred to the interacting parts, can be determined from the following dependence (2):

$$q = f(\mu, \rho, v, t, P) \quad (2)$$

where:

$\mu$  - friction coefficient,

$\rho$  - density of the interacting materials of the couple,  $\text{kg/m}^3$ ,

v - linear velocity,  $\text{m/s}$ ,

t - time of interaction, s,

P - normal load, N.

A linear heat source function was adopted, depending on the friction process parameters. In the calculations, a third-type boundary condition (3) was applied at the contact point: specimen/environment and counter-specimen/environment (the surfaces emit heat to the environment - coefficient  $\alpha=[\text{W}/(\text{m}^2\text{K})]$ ):

$$\alpha(T_{ot} - T_p) = \lambda_p \frac{\partial T_p}{\partial n} \Big|_{pow} \quad (3)$$

where:

$T_p$  and  $T_{ot}$  - surface temperature of the specimen/counter-specimen and ambient temperature,

$\alpha$  - heat exchange coefficient,

$\frac{\partial T_p}{\partial n} \Big|_{pow}$  - projection of the temperature gradient vector against the normal to the surface.

### 4. Calculation results and discussion

Dependence (2) was solved by means of the finite difference method (FDM) using a second-order central difference quotient. A system of linear equations, adequate for the adopted model, was solved by means of FDM according to an explicit scheme. Uniqueness of the solution was obtained for the previously adopted boundary and initial conditions:

$$t=0, T=T_0,=298\text{K}; \quad c=c_0, \quad \lambda=\lambda_0, \quad \rho=\rho_0.$$

The thermophysical properties of the investigated materials are juxtaposed in TABLE 1.

TABLE 1  
Thermophysical properties of the investigated materials

Material Property	TG15	EN-AW AlMg2 (6061)	AHC
Specific heat, c [J/kg*K]	1000	954.2	774-1040
Density, $\rho$ [ $\text{kg/m}^3$ ],	2200	2550	3600
Heat conductivity, $\lambda$ [ $\text{W/m}^*\text{K}$ ]	0.25	184	35.0

Shpenkov [17] and Abdel-Aal [18] found that in the initial period of friction (to 30s), the highest temperature occurs at a certain distance from the friction surface. For this reason, as well as due to the destruction of the thermocouple, the time of measurement was reduced to 30s.

As a result of the numerical calculations, a distribution of the temperature field in the specimen and counter-specimen was obtained for the selected duration time of the process, which is presented in Fig. 4. The nature of the temperature change curves as a function of the interaction time was found to be consistent with the experimental data, which corroborates legitimacy of the adopted model.

The maximum temperature was obtained not on the surface of the interacting parts, but under the surface of a specimen made of TG15 (Fig. 4).

In the specimen made of the TG15 material, there is a characteristic temperature maximum under the surface of the friction zone, at a depth of 0.07 mm, which indicates the existence of an internal heat source.

An increase in temperature under the friction surface in the TG15 specimen results in plasticization of the material and a decrease of its shear strength, thereby increasing the friction coefficient, and contributes to the formation of a sliding film on the surface of the counter-specimen.

The changes in temperature as a function of time  $T=f(t)$  at a point located near the friction zone are presented in Fig. 5

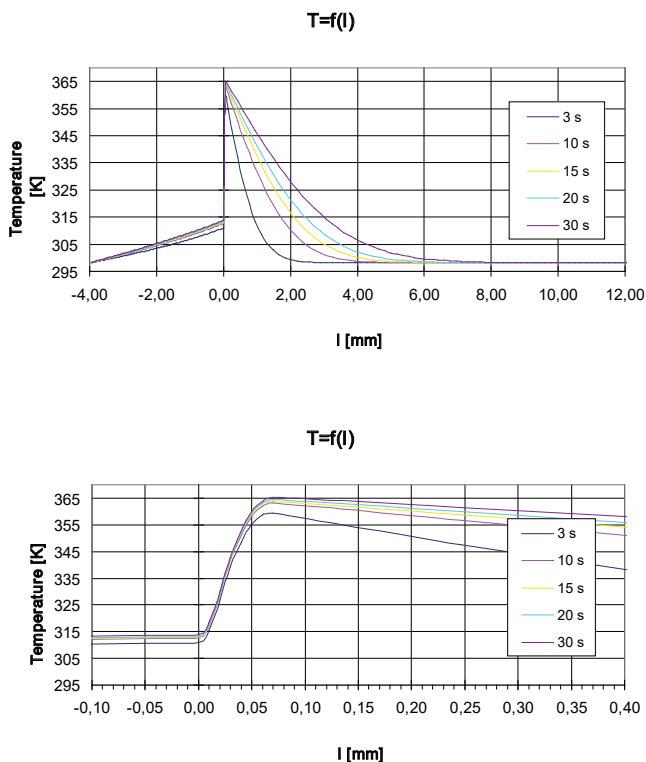


Fig. 4. Changes in temperature in the contact zone as a function of distance from the friction surface ( $l$ ) for a friction time of 3, 10, 15, 20 and 30s, results of modelling (computer simulation)

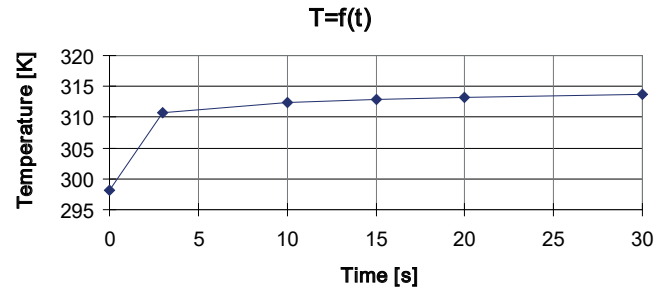


Fig. 5. Changes in temperature ( $T$ ) as a function of the interaction time ( $t$ ) in the counter-specimen (measurement 0.5 mm under the contact surface), experimental results

The results of the experiment and of the numerical simulation are juxtaposed in Fig. 6.

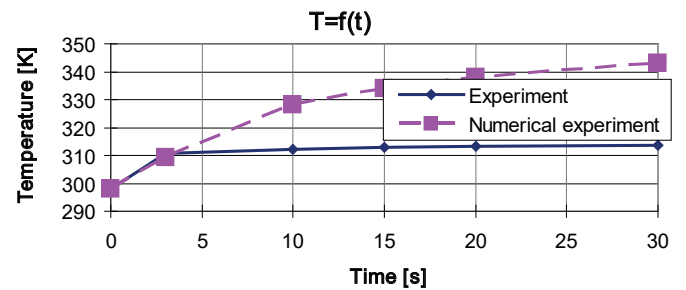


Fig. 6. Changes in temperature ( $T$ ) as a function of the interaction time ( $t$ ) in the counter-specimen (measurement 1 mm under the contact surface), experimental and numerical modelling results

When comparing the numerical simulation results with the experiment, differences in temperatures were found. The discrepancy in the temperatures grows from 1-2 Kelvin at the beginning to 30 K at the end of the test time. Such discrepancies are probably the result of simplification of the model, where the adoption of a one-dimensional system has the greatest influence. In this case the heat is not emitted to the environment through the surface, but instead it is abstracted from some points only.

In addition, stress calculations were made using the finite element method (FEM). It is essential in this method to generate a correct mesh which covers also the very thin AHC layer. The results of the simulation of stresses for the discussed couple allowed the determination of stress distribution in the specimen and counter-specimen (Fig. 7).

Maximum stresses occur in the friction zone and they decrease as the distance from the friction zone increases. There were no maximum stresses observed under or above the surface of interaction. Analysis of stresses obtained as a result of the numerical simulation allowed the localisation of maximum stresses in the neighbourhood of contact of the interacting components. The bigger the distance from the zone of the interaction, the lower the temperature and stresses.

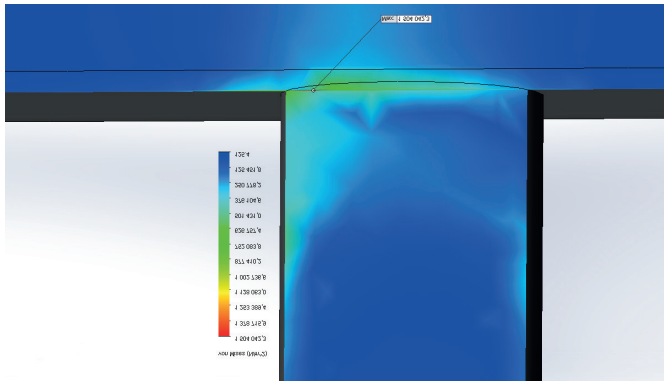


Fig. 7. Computational stress distribution in the investigated couple – friction zone

In the counter-specimen, both the temperature and stresses decrease with an increasing distance from the friction zone. In the TG15 specimen, the maximum temperature occurs at a 0.07 mm distance from the surface of the couple's interaction, while the maximum stress occurs in the friction zone.

The occurrence of the temperature maximum above the friction zone is caused by the presence of internal heat sources in the material of the specimen, which probably results from changes in the polymer structure.

The AHC additionally works as an insulator, thereby causing an increase of temperature in the specimen. It may also cause intensification of polymer destruction and the accompanying heat emission from the newly generated sources.

## 5. Conclusions

The curves of the results of the numerical simulation and of the experiment are consistent in nature. Additionally, the differences in the temperatures are caused by the adoption of constant thermophysical parameters and the assumptions made, as well as the omission of the influence of roughness parameters and energy dissipation.

In a further stage, the numerical experiment should be conducted in a 2D space, while taking account of variable thermophysical parameters (to be determined experimentally). The taking into account of variable thermophysical parameters and making calculations in a 2D system will enable obtaining lower temperatures from the modelling, and thus smaller differences between the results obtained from the experiment and calculated numerically.

The FEM stress analysis did not allow the observation of maximum stresses under the surface of the interacting tribological couple.

The results of numerical calculations depend on the method applied and on the possibilities of adjusting commercial programmes to the real conditions of the conducted experiment. Therefore, it seems purposeful to further develop

the original software which enables taking into account of the real conditions of the interaction of the tribological couple.

## REFERENCES

- [1] M.D. Roehrl, *Piston for Internal Combustion Engines*, Verlag Moderne Industrie, Augsburg (2002).
- [2] J. Korzekwa, W. Skoneczny, G. Dercz, *Wear Mechanism of Al<sub>2</sub>O<sub>3</sub>/WS<sub>2</sub> With PEEK/BG Plastic*, *Journal of Tribology-Transactions of the ASME* **136** (1), (2014).
- [3] T. Kmita, M. Bara, *Surface oxide layers with an increased carbon content for applications in oil-less tribological systems*. *Chemical and process engineering* **33** (3), 479-486, (2012).
- [4] A. Posmyk, H. Wistuba, *The ceramic composite coatings with glassy nano-carbon*, *Composites* **1**, 31-35 (2008).
- [5] *Grafit Prasowany w Zastosowaniach Przemysłowych*. Karta wyrobu Firma ATK s.c., Kraków (2013).
- [6] J. Myalski, *Polimerowe materiały ślizgowe do pracy w podwyższonej temperaturze*. *Problemy eksploatacji*, **2**, 113-122 (2010).
- [7] *Beyond Performance Plastics*. Catalogue 3P Inc., Huston USA (2015).
- [8] W. Skoneczny, *Monografia, Kształtowanie wybranych właściwości warstw powierzchniowych na bazie tlenku aluminium*. ATH, Bielska-Biała (2009).
- [9] G. Służałek, P. Duda, H. Wistuba, *Tribological Characteristics of Anodic Oxide Coat (AOC) Modified - Sealed up the Polymer*; *Journal: Solid State of Phenomena*; **199**; 209 – 216, (2013).
- [10] M. Kuciek, *Analityczne modele nieustalonego nagrzewania tarcowego*, Publishing house: Politechnika Białostocka, (2012).
- [11] W. Wieleba, *Analiza procesów tribologicznych zachodzących podczas współpracy kompozytów PTFE ze stałą*, Oficyna Wydawnicza Politechniki Wrocławskiej, Wrocław (2002).
- [12] H. Kochanek, J. Sadowski, *Zagadnienie wpływu zużycia na pole temperatury pary tarcowej*, *Tribologia*, **1**, 73-84, (2012).
- [13] Q. Liu Wang, *A three-dimensional thermomechanical model of contact between non-conforming rough surfaces*. *ASME Journal of Tribology* **123**, 17-26. (2001).
- [14] N. Laraqi, *Phenomene de construction thermique dans les contacts*, *International Journal of Heat and Mass Transfer* **39**, 17, 3717-3724, (1996).
- [15] M. Mochnacki, J.S. Suchy, *Numerical methods in computations of foundry processes*, Polish Foundrymen's Technical Association, (1995), Cracow, PFTA
- [16] S. Wiśniewski, T.S. Wiśniewski, *Wymiana ciepła*, WNT, (2000).
- [17] G.P. Shpenkov, *Friction surface phenomena*, Elsevier, Amsterdam, (1995).
- [18] H.A. Adbel-Aal: *On the bulk temperatures of dry rubbing metallic solid pairs*, *International Comm. in Heat and Mass Transfer* **26**, 4, 587-596, (1999).

